

## Minimum energy paths for dislocation nucleation in strained epitaxial layers

O. Trushin,<sup>1,4</sup> E. Granato,<sup>2,3</sup> S. C. Ying,<sup>3</sup> P. Salo,<sup>4</sup> and T. Ala-Nissila<sup>3,4</sup>

<sup>1</sup>*Institute of Microelectronics and Informatics, Academy of Sciences of Russia, Yaroslavl 150007, Russia*

<sup>2</sup>*Laboratório Associado de Sensores e Materiais, Instituto Nacional de Pesquisas Espaciais, 12201-970 São José dos Campos, SP Brasil*

<sup>3</sup>*Department of Physics, Brown University, Providence, Rhode Island 02912*

<sup>4</sup>*Helsinki Institute of Physics and Laboratory of Physics, Helsinki University of Technology, FIN-02015 HUT, Espoo, Finland*

(Received 29 April 2002; published 24 June 2002)

We study numerically the minimum energy path and energy barriers for dislocation nucleation in a two-dimensional atomistic model of strained epitaxial layers on a substrate with lattice misfit. Stress relaxation processes from coherent to incoherent states for different transition paths are determined using saddle point search based on a combination of repulsive potential minimization and the Nudged Elastic Band method. The minimum energy barrier leading to a final state with a single misfit dislocation nucleation is determined. A strong tensile-compressive asymmetry is observed. This asymmetry can be understood in terms of the qualitatively different transition paths for the tensile and compressive strains.

DOI: 10.1103/PhysRevB.65.241408

PACS number(s): 68.55.Ac, 68.35.Gy, 68.90.+g

The growth and stability of heteroepitaxial overlayers is one of the central problems in current materials science. Energy-balance arguments for the competition between strain energy buildup and strain relief due to dislocation nucleation in mismatched epitaxial films lead to the concept of an equilibrium critical thickness. This is defined as the thickness at which the energy of the epitaxial state is equal to that of a state containing a single misfit dislocation.<sup>1</sup> The predicted critical value from this equilibrium consideration however, both from continuous elastic models<sup>2,3</sup> and from models incorporating layer discreteness,<sup>4</sup> is much smaller than the observed experimental value for the breakdown of the epitaxial state. This suggests that the defect-free (coherent) state above the equilibrium critical thickness is metastable<sup>5</sup> and the rate of dislocation generation is actually controlled by kinetic considerations. The idea of strain relaxation as an activated process is supported by experimental results for the temperature dependence of the critical thickness.<sup>5,6</sup> It is also the fundamental assumption in kinetic semiempirical models.<sup>7</sup>

Physically, it is expected that the lowest energy barrier for the nucleation of dislocations would correspond to a path that initiates from the free surface (with or without defects). Such processes have been considered in a number of studies within continuum models.<sup>8-10</sup> It has been pointed out that surface steps and surface roughness that are not included in the continuum model could play an important role for dislocation nucleation.<sup>11-14</sup> Thus, atomistic study is important for a detailed understanding and direct determination of the mechanisms for defect nucleation in epitaxial films. However, determination of the correct transition path and the nucleation barrier from the initial coherent state to the final state with misfit dislocations is an extremely challenging problem in an atomistic model. There are many saddle points and transition paths in the neighborhood of the initial coherent state. A brute force molecular dynamics (MD) study is impractical because of the rare event nature of the activated processes. In recent years, great progress has been made in the general field of search for transition paths for compli-

cated energy landscapes.<sup>15,16</sup> In addition, various accelerated hyperdynamics schemes<sup>17,18</sup> have been developed to overcome the computational problems for rare events. However, these schemes still involve considerable computational efforts for complicated, large energy barriers and often require a qualitative picture of the energy landscape as a starting point. Recently we have developed a repulsive potential minimization method<sup>19</sup> which allows automatic generation of many paths leading away from the initial minimum energy coherent state. When combined with the Nudged Elastic Band method (NEB),<sup>15</sup> this method can be used to efficiently locate saddle point configurations and barriers for each transition path without having to make any specific assumptions about the nature of the transition path.

For the present study, we consider a two-dimensional model of the epitaxial film and substrate where the atomic layers are confined to a plane as illustrated in Fig. 1(a). Interactions between atoms in the system are modelled by a generalized Lennard-Jones pair potential,<sup>20</sup> that is modified to insure that the potential and its first derivative vanish<sup>11</sup> at a cut-off distance  $r_c$  as

$$U(r) = V(r), \quad r \leq r_0;$$

$$U(r) = V(r) \left[ 3 \left( \frac{r_c - r}{r_c - r_0} \right)^2 - 2 \left( \frac{r_c - r}{r_c - r_0} \right)^3 \right], \quad r > r_0, \quad (1)$$

where

$$V(r) = \varepsilon \left[ \frac{m}{n-m} \left( \frac{r_0}{r} \right)^n - \frac{n}{n-m} \left( \frac{r_0}{r} \right)^m \right], \quad (2)$$

and  $r$  is the interatomic distance,  $\varepsilon$  the dissociation energy, and  $r_0$  the equilibrium distance between the atoms. This potential has been used previously,<sup>11</sup> with  $n = 12$  and  $m = 6$ , in a Monte Carlo simulation of epitaxial growth. We have chosen the value  $n = 8$  and  $m = 5$  for the present study. In contrast to the standard 6-12 potential, this 5-8 potential has a slower fall-off. Thus, when combined with the variation of the cutoff radius  $r_c$ , this choice allows us to systematically

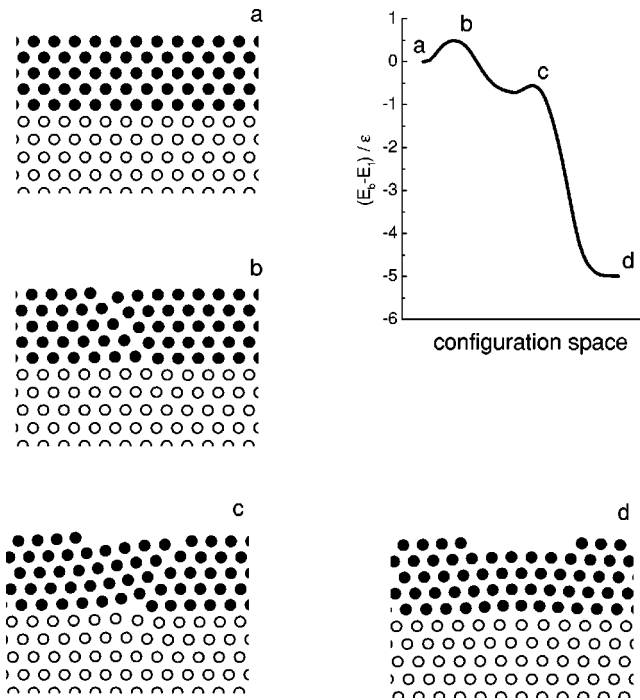


FIG. 1. Particle configurations and energy change  $E_i - E_0$  at different states (images) along the minimum energy path, for tensile strain ( $f = -8\%$ ). The two layers at the bottom are held fixed while all others are free to move. Open circles represent the substrate atoms and filled circles the epitaxial film. Only the central part of the layers with major atom rearrangements is shown.

study the effect of the range of the potential on misfit dislocation. Also, the 5–8 potential gives a more realistic description of metallic systems than the 6–12 case. The equilibrium interatomic distance  $r_0$  was set to different values for the substrate, epitaxial film, and the substrate-film interfaces. The substrate  $r_0 = r_{ss}$  and the epitaxial film  $r_0 = r_{ff}$  parameters were varied to give a misfit  $f$  between lattice parameters as  $f = (r_{ff} - r_{ss})/r_{ss}$ . For the film-substrate interaction we set the equilibrium distance as the average of the film and substrate lattice constants,  $r_0 = r_{fs} = (r_{ff} + r_{ss})/2$ . Positive misfit  $f$  corresponds to compressive strain and negative  $f$  to tensile strain when the film is coherent with the substrate. Calculations were performed with periodic boundary conditions in the direction parallel to the film-substrate interface. Typically, one-dimensional layers containing 50 atoms or more were used in the calculations. In the calculations the bottom five layers represented the substrate, with the last two layers held fixed to simulate a semi-infinite substrate while all other layers were free to move.

Our proposed scheme of identifying the saddle points and the transition paths consists of several stages. First, the initial epitaxial state is prepared by minimizing the total energy of the system using MD cooling. This leads to an initial coherent epitaxial state in which the interlayer spacing is relaxed, but the atoms within the layers are under compressive or tensile strain according to the misfit. Next, we introduce a short-ranged repulsive potential centered at the starting epitaxial configuration of the form

$$U_{tot}(r) = U(r) + A \exp\{-\alpha(r - r_0)^2\}, \quad (3)$$

where  $r_0$ 's are the coordinates of the initial state at the minimum.<sup>16</sup> The basic idea here is to modify the local energy surface to make the initial epitaxial state unstable. When the system is slightly displaced from the initial state (randomly or in a selective way), it will then be forced to move to nearby minimum energy states. By making this repulsive potential sufficiently localized around the initial potential minima, the surrounding minima would be unaffected and the final state energy would then depend only on the true potential of the system. This method can generate many different final states depending on both the initial displacements and the parameters of the repulsive potential. In this Rapid Communication, we only consider final configurations corresponding to a single misfit dislocation. Rather than trying random initial displacements, some knowledge of the dislocation generation mechanism is useful for expediting the process. Given the knowledge of the final state, we then use the NEB method to locate the saddle point and find the minimum energy path (MEP) between the initial and final states. We note that the path generated in the first part of moving away from the repulsive potential can be used as an initial guess for the MEP determination in the NEB method.

We have performed calculations for various misfits, but in this Rapid Communication we concentrate on the case of a relatively large 8% misfit. We work with dimensionless quantities with  $\epsilon$  as the energy scale and  $r_{ss}$  as the length scale. Two different choices of cutoff, namely  $r_c = 1.5 r_{ss}$  and  $r_c = 4.7 r_{ss}$  were made. The results for the barriers are qualitatively similar, so we present here only the results for the short range potential with  $r_c = 1.5 r_{ss}$ . However, the equilib-

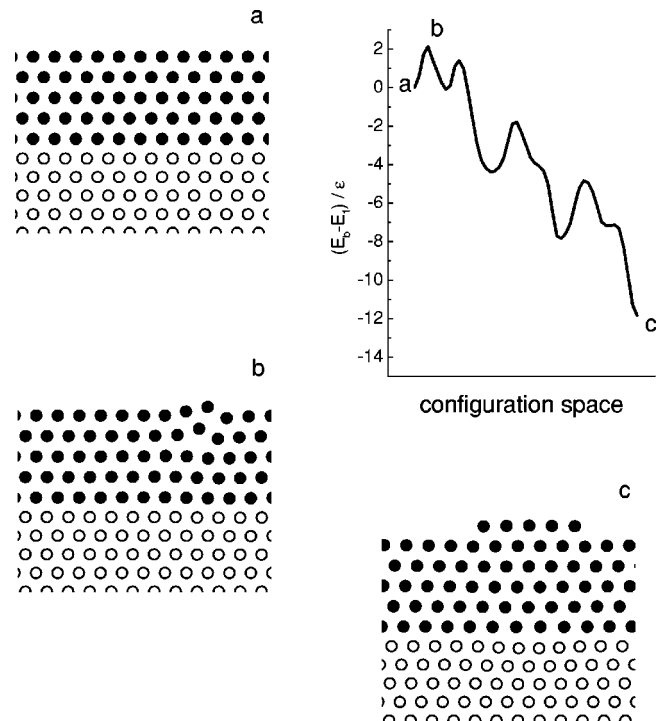


FIG. 2. Same as Fig. 1 but for compressive strain ( $f = +8\%$ ).

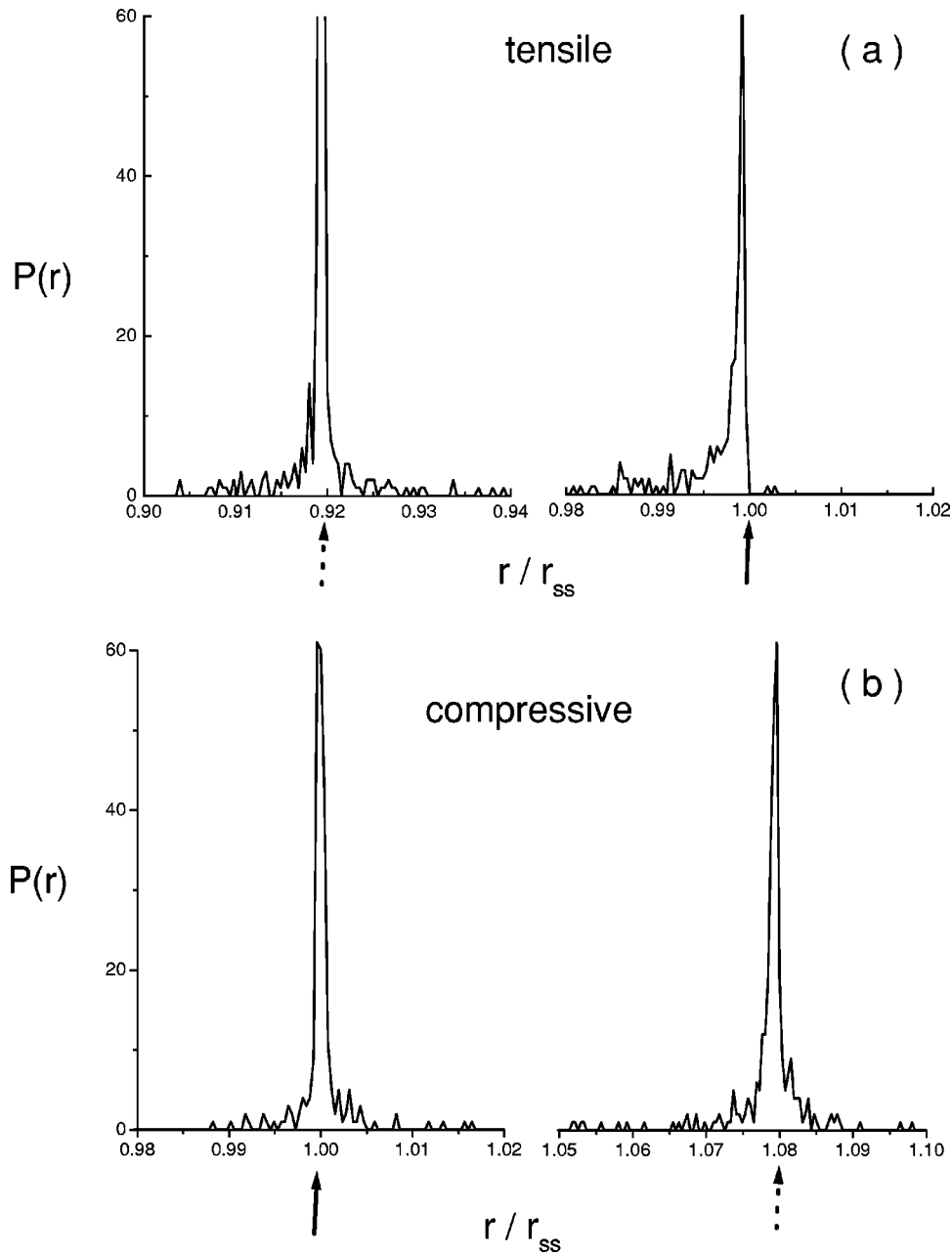


FIG. 3. Nearest-neighbor bond distributions of the epitaxial film at the saddle point for the (a) tensile, and (b) compressive cases. Solid and dotted arrows indicate the position of the delta-function peak corresponding to intralayer and interlayer bond distributions of the initial coherent film.

rium critical thickness and its asymmetry with respect to tensile or compressive strain are very sensitive to the range of the potential.<sup>19</sup>

The results for the MEP from coherent to incoherent states are shown in Fig. 1 for a film under tensile strain and Fig. 2 for compressive strain. They show clearly the existence of an energy barrier for the nucleation of a misfit dislocation. Thus, the nonequilibrium critical thickness can be much larger than the equilibrium value and it is controlled in practice by the kinetics of defect nucleation.

For compressive strain, the final state is characterized by the presence of an adatom island on the surface of the film for each misfit dislocation. The number of adatoms in the island exactly corresponds to the number of layers in the film. Such form of the final state is determined by the geometry of the misfit dislocation. For every misfit dislocation, an

extra atom is removed from each layer to relieve the compressive stress. For tensile strain, the final state is characterized by the presence of pits on the surface. Again, the size of the pit is determined by geometrical considerations. For every misfit dislocation, an extra atom has to be added to each layer to relieve the tensile stress. For both cases, the dislocation core is localized in the substrate-film interface region.

Figures 1 and 2 also show the particle configurations at the different points along the MEP which reveal details of defect nucleation and strain relaxation process. The transition path for the compressive strain has a more local nature, with relatively fewer bonds involved initially, whereas for the tensile strained film, the nucleation proceeds via a more collective path, involving concerted motion along glide planes. The energy barrier for nucleation of a dislocation is much higher for the compressive strain relative to the case of tensile

strain. This asymmetry is very robust and it persists when we change the range of the potential by varying the cutoff.

To understand the origin of this asymmetry, we plot in Fig. 3 the distribution of the nearest-neighbor bond lengths for the film from the initial epitaxial film to the saddle point configuration for both the compressive and tensile cases. It can be seen that the behavior of the compressively strained film and the tensile-strained film is very different. In the tensile case, the redistribution of the bond lengths going from the initial coherent state to the saddle point configuration involves a significant contraction of the intralayer bonds leading to partial relaxation of the tensile strain in the film. On the other hand, for the compressively strained film, the initial delta function peak for the intralayer bond lengths broadens almost symmetrically and there are no significant relaxation of the compressive strain in the film. This explains the relatively higher energy costs and a corresponding larger nucleation barrier for the compressive strained film. Microscopically, the origin of the different behavior could arise from the strong anharmonicity of the interaction potential. For the compressive strain, intralayer rearrangements involve some further compression of the bonds which is energetically costly. Thus, a more localized initial configuration with a higher barrier results as opposed to the collective behavior of the tensile strained layer. We have also checked that the boundary conditions and system sizes do not affect the results qualitatively by comparing results from systems with

periodic and free boundary conditions, and for layers twice as long.

In summary, we have developed a new scheme of identifying minimal energy path for spontaneous generation of misfit dislocation in an epitaxial film. This approach requires no *a priori* assumptions about the nature of the transition path or the final states. A nonzero activation barrier for dislocation nucleation is found in the minimum energy path from coherent to incoherent state above the equilibrium critical thickness, confirming the metastability of the epitaxial coherent film. The nucleation mechanism from a flat surface depends crucially on whether we start from a tensile or compressive initial state of the film. This asymmetry originates from the anharmonicity of the interaction potentials which leads to qualitatively different transition paths for the two types of strains. A tensile-compressive asymmetry has also been found previously<sup>11,12</sup> in other contexts. The present method can be extended to three-dimensional models with more realistic interaction potentials. Preliminary calculations for the Pd/Cu and Cu/Pd systems<sup>19</sup> with the Embedded Atom Model potentials<sup>21</sup> confirms the effectiveness of the method in three dimensions. These results will be published elsewhere.

This work was supported by a NSF-CNPq grant (E.G. and S.C.Y.), by the Russian Ministry of Science and Technology (O.T.), FAPESP (E.G.), and by the Academy of Finland through its Center of Excellence program (O.T., P.S., and T.A-N.).

<sup>1</sup>J.C. Bean, *Science* **230**, 127 (1985).

<sup>2</sup>J.W. Matthews and A.E. Blakeslee, *J. Cryst. Growth* **27**, 118 (1974).

<sup>3</sup>C.A.B. Ball and J.H. van der Merwe, in *Dislocation in Solids*, edited by F.R.N. Nabarro (North-Holland, Amsterdam, 1983).

<sup>4</sup>E. Granato, J.M. Kosterlitz, and S.C. Ying, *Phys. Rev. B* **39**, 3185 (1989).

<sup>5</sup>J.Y. Tsao, B.W. Dodson, S.T. Picraux, and D.M. Cornelison, *Phys. Rev. Lett.* **59**, 2455 (1987).

<sup>6</sup>J. Zou and D.J.H. Cockayne, and B.F. Usher, *Appl. Phys. Lett.* **68**, 673 (1996).

<sup>7</sup>D.C. Houghton, *J. Appl. Phys.* **70**, 2136 (1991).

<sup>8</sup>B.J. Spencer, P.W. Voorhees, and S.H. Davis, *Phys. Rev. Lett.* **67**, 3696 (1991).

<sup>9</sup>A.G. Cullis, A.J. Pidduck, and M.T. Emeny, *Phys. Rev. Lett.* **75**, 2368 (1995).

<sup>10</sup>J. Grilhé, *Europhys. Lett.* **23**, 141 (1993).

<sup>11</sup>L. Dong, J. Schnitker, R.W. Smith, and D.J. Srolovitz, *J. Appl. Phys.* **83**, 217 (1998).

<sup>12</sup>M. Ichimura and J. Narayan, *Philos. Mag. A* **72**, 281 (1995).

<sup>13</sup>J. Tersoff and F.K. LeGoues, *Phys. Rev. Lett.* **72**, 3570 (1994).

<sup>14</sup>S. Brochard, P. Beauchamp, and J. Grilhé, *Philos. Mag. A* **80**, 503 (2000).

<sup>15</sup>H. Jonsson, G. Mills and K.W. Jacobsen, in *Classical and Quantum Dynamics in Condensed Phase Simulations*, edited by B. J. Berne *et al.* (World Scientific, Singapore, 1998).

<sup>16</sup>N. Mousseau and G.T. Barkema, *Phys. Rev. B* **61**, 1898 (2000).

<sup>17</sup>A.F. Voter, *Phys. Rev. Lett.* **78**, 3908 (1997); *J. Chem. Phys.* **106**, 4665 (1997).

<sup>18</sup>A. Sorensen and A.F. Voter, *J. Chem. Phys.* **112**, 9599 (2000).

<sup>19</sup>O. Trushin *et al.* (unpublished).

<sup>20</sup>S. Zhen and G.J. Davies, *Phys. Status Solidi A* **78**, 595 (1983).

<sup>21</sup>S.M. Foiles, M.I. Baskes, and M.S. Daw, *Phys. Rev. B* **33**, 7983 (1986).